Reinforcement Learning-Based Design of Side-Channel Countermeasures

Rijsdijk, Jorai; Wu, Lichao; Perin, Guilherme

DOI
10.1007/978-3-030-95085-9_9

Publication date
2022

Document Version
Final published version

Published in
Security, Privacy, and Applied Cryptography Engineering

Citation (APA)
Rijsdijk, J., Wu, L., & Perin, G. (2022). Reinforcement Learning-Based Design of Side-Channel Countermeasures. In L. Batina, S. Picek, S. Picek, & M. Mondal (Eds.), *Security, Privacy, and Applied Cryptography Engineering : 11th International Conference, SPACE 2021, Proceedings* (1 ed., pp. 168-187). (Lecture Notes in Computer Science (including subseries Lecture Notes in Artificial Intelligence and Lecture Notes in Bioinformatics); Vol. 13162). Springer. https://doi.org/10.1007/978-3-030-95085-9_9

Reinforcement Learning-Based Design of Side-Channel Countermeasures

Jorai Rijsdijk, Lichao Wu(✉), and Guilherme Perin

Delft University of Technology, Delft, The Netherlands

Abstract. Deep learning-based side-channel attacks are capable of breaking targets protected with countermeasures. The constant progress in the last few years makes the attacks more powerful, requiring fewer traces to break a target. Unfortunately, to protect against such attacks, we still rely solely on methods developed to protect against generic attacks. The works considering the protection perspective are few and usually based on the adversarial examples concepts, which are not always easy to translate to real-world hardware implementations.

In this work, we ask whether we can develop combinations of countermeasures that protect against side-channel attacks. We consider several widely adopted hiding countermeasures and use the reinforcement learning paradigm to design specific countermeasures that show resilience against deep learning-based side-channel attacks. Our results show that it is possible to significantly enhance the target resilience to a point where deep learning-based attacks cannot obtain secret information. At the same time, we consider the cost of implementing such countermeasures to balance security and implementation costs. The optimal countermeasure combinations can serve as development guidelines for real-world hardware/software-based protection schemes.

Keywords: Side-channel analysis · Reinforcement learning · Countermeasures · Deep learning

1 Introduction

Deep learning is a very powerful option for profiling side-channel analysis (SCA). In profiling SCA, we assume an adversary with access to a clone device under attack. Using that clone device, the attacker builds a model that is used to attack the target. This scenario maps perfectly to supervised machine learning, where first, a model is trained (profiling phase) and then tested on previously unseen examples (attack phase). While other machine learning approaches also work well in profiling SCA (e.g., random forest or support vector machines), deep learning (deep neural networks) is commonly considered the most powerful direction. This is because deep neural networks 1) do not require feature engineering, which means we can use raw traces, and 2) can break protected implementations, which seems to be much more difficult with simpler machine learning techniques

L. Batina et al. (Eds.): SPACE 2021, LNCS 13162, pp. 168–187, 2022.
https://doi.org/10.1007/978-3-030-95085-9_9

or the template attack [17]. As such, the last few years brought several research works that report excellent attack performance and breaking of targets in a (commonly) few hundred attack traces. What is more, attack improvements are regularly appearing as many new results from the machine learning domain can be straightforwardly applied to improve the side-channel attacks, see, e.g., [16, 19, 25]. Simultaneously, there are only sporadic improvements from the defense perspective, and almost no research aimed to protect against deep learning-based SCA.

We consider this an important research direction. If deep learning attacks are the most powerful ones, an intuitive direction should be to design countermeasures against such attacks. Unfortunately, this is also a much more difficult research perspective. We can find several reasons for it:

- As other domains do not consider countermeasures in the same shape as in SCA, it is not straightforward to use the knowledge from other domains.
- While adversarial machine learning is an active research direction and intuitively, adversarial examples are a good defense against deep learning-based SCA, it is far from trivial to envision how such defenses would be implemented in cryptographic hardware. Additionally, adversarial examples commonly work in the amplitude domain but not in the time domain.
- It can be easier to attack than to defend in the context of masking and hiding countermeasures. Validating that an attack is successful is straightforward as it requires assessing how many attack traces are needed to break the implementation. Unfortunately, confirming that a countermeasure works would, in an ideal case, require testing against all possible attacks (which is not possible).

There are only a few works considering countermeasures against machine learning-based SCA to the best of our knowledge. Inci et al. used adversarial learning as a defensive tool to obfuscate and mask side-channel information (concerning micro-architectural attacks) [9]. Picek et al. considered adversarial examples as a defense against power and EM side-channel attacks [18]. While they reported the defense works, how would such a countermeasure be implemented is still unknown. Gu et al. used an adversarial-based countermeasure that inserts noise instructions into code [7]. The authors report that their approach also works against classical side-channel attacks. However, such a countermeasure cannot be implemented at zero cost. From a designer's perspective, knowing the trade-off between the countermeasures' complexity and target's performance (i.e., running speed and power consumption), the countermeasure should be carefully selected and tuned. Finally, Van Ouytsel et al. recently proposed an approach they called cheating labels, which would be misleading labels that the device is trying to make obvious to the classifier [13]. Differing from the previous listed works, this work aimed at showing the limitations analysis in the SCA context, regardless of the specific technique.

In this work, we do not aim at finding a more powerful countermeasure with adversarial examples. Instead, with the help of the reinforcement learning paradigm, our goal is to find an optimal combination of hiding countermeasures that have the lowest performance cost but still ensure that the deep learning-based SCA is difficult to succeed. Although the random search can reach similar goals, we argue that our SCA-optimized reinforcement learning method can consistently evolve the countermeasure selection, thus outputs reliable results. We emphasize that we simulate the countermeasures to assess their influence on a dataset. This is why we concentrate on hiding countermeasures, as it is easier to simulate hiding than masking (and there are also more options, making the selection more challenging). As we attack datasets that are already protected with masking, we consider both countermeasure categories covered. What we provide is an additional layer of resilience besides the masking countermeasure. The optimized combinations of countermeasures work in both amplitude and time domains and could be easily implemented in real-world targets. From a developer's perspective, the optimized combination can become the development guideline of protection mechanisms. In this paper, we conduct experiments with results indicating the time-based countermeasures as the key ingredient of strong resilience against deep learning-based SCA. Our main contributions are:

1. We propose a novel reinforcement learning approach to construct low-cost hiding countermeasure combinations, making deep learning-based SCA difficult to succeed.
2. We motivate and develop custom reward functions for countermeasure selection to increase the SCA resilience.
3. We conduct extensive experimental analysis considering four countermeasures, two datasets, and two leakage models.
4. We report on a number of countermeasures that indicate strong resilience against the selected profiling SCAs.

2 Preliminaries

Calligraphic letters ($\mathcal{X}$) denote sets and the corresponding upper-case letters (X) random variables and random vectors $\mathbf{X}$ over $\mathcal{X}$. The corresponding lower-case letters x and $\mathbf{x}$ denote realizations of X and $\mathbf{X}$, respectively. A dataset $\mathbf{T}$ is a collection of traces (measurements). Each trace $\mathbf{t}_i$ is associated with an input value (plaintext or ciphertext) $\mathbf{d}_i$ and a key candidate $\mathbf{k}_i$. Here, $k \in \mathcal{K}$ and k^* represents the correct key. As common in profiling SCA, we divide the dataset into three parts: a profiling set of N traces, a validation set of V traces, and an attack set of Q traces.

2.1 Deep Learning and Profiling Side-Channel Analysis

We consider the supervised learning task where the goal is to learn a function f that maps an input to the output ($f : \mathcal{X} \rightarrow Y$)) based on examples of input-output pairs. There is a natural mapping between supervised learning and profiling SCA. Supervised learning has two phases: training and test. The training phase corresponds to the SCA profiling phase, and the testing phase corresponds to the side-channel attack phase. The profiling SCA runs under the following setup:

- The goal of the profiling phase is to learn the parameters of the profiling model minimizing the empirical risk represented by a loss function on a profiling set of size N.
- The goal of the attack phase is to make predictions about the classes $y(x_1, k^*), \ldots, y(x_Q, k^*)$, where k^* represents the secret (unknown) key on the device under the attack.

Probabilistic deep learning algorithms output a matrix that denotes the probability that a certain measurement should be classified into a specific class. Thus, the result is a matrix P with dimensions equal to $Q \times c$, where c denotes the number of output labels (classes). The probability $S(k)$ for any key candidate k is the maximum log-likelihood distinguisher:

$$S(k) = \sum_{i=1}^{Q} \log(\mathbf{p}_{i,v}). \tag{1}$$

The value $\mathbf{p}_{i,v}$ represents the probability that a specific class v is predicted. The class v is obtained from the key and input through a cryptographic function and a leakage model.

From the matrix P, it is straightforward to obtain the accuracy of the model f. Still, in SCA, an adversary is not interested in predicting the classes in the attack phase but in obtaining the secret key k^*. Thus, to estimate the difficulty of breaking the target, it is common to use metrics like guessing entropy (GE) [21].

Given Q traces in the attack phase, an attack outputs a key guessing vector $\mathbf{g} = [g_1, g_2, \ldots, g_{|\mathcal{K}|}]$ in decreasing order of probability (g_1 is the most likely key candidate and $g_{|\mathcal{K}|}$ the least likely key candidate). Guessing entropy represents the average position of k^* in $\mathbf{g}$.

2.2 Side-Channel Countermeasures

It is common to protect the implementation with countermeasures. Countermeasures aim to break the statistical link between intermediate values and traces (e.g., power consumption or EM emanation). There are two main categories of countermeasures for SCA: masking and hiding. In many cases, they will be both implemented in increase the security level of the product.

In masking, a random mask is generated to conceal every intermediate value. More precisely, random masks are used to remove the correlation between the measurements and the secret data. In general, there are two types of masking: Boolean masking and arithmetic masking.

On the other hand, the goal of hiding is to make measurements looking random or constant. Hiding decreases the signal-to-noise ratio (SNR) only. Hiding can happen in the amplitude (e.g., adding noise) and time (e.g., desynchronization, random delay interrupts, jitter) dimensions. In our work, we simulate only hiding countermeasures as masking is always active.

2.3 Datasets and Leakage Models

The two datasets we use are versions of the ASCAD database [2]. Both datasets contain the measurements from an 8-bit AVR microcontroller running a masked AES-128 implementation. We attack the first masked key byte (key byte three). The datasets are available at https://github.com/ANSSI-FR/ASCAD. The first dataset version has a fixed key (thus, the key is the same in the profiling and attack set). This dataset consists of 50 000 traces for profiling and 10 000 for the attack. From 50 000 traces in the profiling set, we use 45 000 traces for profiling and 5 000 for validation. Each trace has 700 features (preselected window). The second version has random keys, with 200 000 traces for profiling and 100 000 for the attack. We use 5 000 traces from the attack set for validation (note that the attack set has a fixed but a different key from the profiling set). Each trace has 1 400 features (preselected window).

We consider two leakage models:

- The Hamming weight (HW) leakage model - the attacker assumes the leakage proportional to the sensitive variable's Hamming weight. Considering the AES cipher with 8-bit S-boxes, this leakage model has nine classes for a single key byte (values from 0 to 8).
- The Identity (ID) leakage model - the attacker considers the leakage in the form of an intermediate value of the cipher. Considering the AES cipher with 8-bit S-boxes, this leakage model results in 256 classes for a single key byte (values from 0 to 255).

2.4 Reinforcement Learning

Reinforcement learning (RL) aims to teach an agent how to perform a task by letting the agent experiment and experience the environment. There are two main categories of reinforcement learning algorithms: policy-based algorithms and value-based algorithms. Policy-based algorithms directly try to find this optimal policy. Value-based algorithms, however, try to approximate or find the value function that assigns state-action pairs a reward value. Most reinforcement learning algorithms are centered around estimating value functions, but this is not a strict requirement for reinforcement learning. For example, methods such as genetic algorithms or simulated annealing can all be used for reinforcement learning without ever estimating value functions [22]. In this research, we only focus on Q-Learning, belonging to the value estimation category.

Reinforcement learning has fundamental differences compared with supervised and unsupervised machine learning, commonly adopted by the SCA community. Supervised machine learning learns from a set of examples (input-output pairs) labeled with the correct answers. A benefit of reinforcement learning over supervised machine learning is that the reward signal can be constructed without prior knowledge of the correct course of action, which is especially useful if such a dataset does not exist or is infeasible to obtain. In unsupervised machine learning, the algorithm attempts to find some (hidden) structure within a dataset, while reinforcement learning aims to teach an agent how to perform a task through rewards and experiments [22].

Q-Learning. Q-Learning was introduced in 1989 by Chris Watkins [23] with an aim not only to learn from the outcome of a set of state-action transitions but from each of them individually. Q-learning is a value-based algorithm that tries to estimate $q_*(s, a)$, the reward of taking action a in the state s under the optimal policy, by iteratively updating its stored q-value estimations using Eq. (2). The simplest form of Q-learning stores these q-value estimations as a simple lookup table and initializes them with some chosen value or method. This form of Q-learning is also called Tabular Q-learning.

Equation (2) is used to incorporate the obtained reward into the saved reward for the current state R_t. S_t and A_t are the state and action at time t, and $Q(S_t, A_t)$ is the current expected reward for taking action A_t in state S_t. α and γ are the q-learning rate and discount factor, which are hyperparameters of the Q-learning algorithm. The q-learning rate determines how quickly new information is learned, while the discount factor determines how much value to assign to short-term versus long-term rewards. R_{t+1} is the currently observed reward for having taken action A_t in state S_t. $max_a Q(S_{t+1}, a)$ is the maximum of the expected reward of all the actions a that can be taken in state S_{t+1}.

$$Q(S_t, A_t) \leftarrow Q(S_t, A_t) + \alpha \left[R_{t+1} + \gamma \max_a Q(S_{t+1}, a) - Q(S_t, A_t) \right]. \quad (2)$$

3 Related Works

We divide related works into two directions: improving deep learning-based SCA and improving the defenses against such attacks. In the first direction, from 2016 and the first paper using convolutional neural networks [11], there are continuous improvements in the attack performance. Commonly, such works investigate (note this is only a small selection of the papers):

– **the importance of hyperparameters and designing top-performing neural networks**. Benadjila et al. made an empirical evaluation of different CNN hyperparameters for the ASCAD dataset [2]. Perin and Picek explored the various optimizer choices for deep learning-based SCA [15]. Zaid et al. proposed a methodology to select hyperparameters related to the size of layers in CNNs [29]. To the best of our knowledge, this is the first methodology to build CNNs for SCA. Wouters et al. [24] improved upon the work from Zaid et al. [29] and showed it is possible to reach similar attack performance with significantly smaller neural network architectures. Wu et al. used Bayesian optimization to find optimal hyperparameters for multilayer perceptron and convolutional neural network architectures [25]. Rijsdijk et al. used reinforcement learning to design CNNs that exhibit strong attack performance and have a small number of trainable parameters [20]. Our reinforcement learning setup is inspired by the one presented here, especially the reward function

part[1] To improve the attack performance, some authors also proposed custom elements for neural networks for SCA. For instance, Zaid et al. [28], and Zhang et al. [30] introduced new loss functions that improve the attack performance.
- **well-known techniques from the machine learning domain to improve the performance of deep learning-based attacks**. Cagli et al. showed how CNNs could defeat jitter countermeasure, and they used data augmentation to improve the attack process [3]. Kim et al. constructed VGG-like architecture that performs well over several datasets, and they use regularization in the form of noise added to the input [10]. Perin et al. showed how ensembles could improve the attack performance even when single models are only moderately successful [14]. Wu et al. used the denoising autoencoder to remove the countermeasures from measurements to improve the attack performance [26]. Perin et al. considered the pruning technique and the lottery ticket hypothesis to make small neural networks reach top attack performance [16].
- **explainability and interpretability of results**. Hettwer et al. investigated how to select points of interest for deep learning by using three deep neural network attribution methods [8]. Masure et al. used gradient visualization to discover where the sensitive information leaks [12].

On the other hand, the domain of countermeasures' design against machine learning-based SCA is much less explored[2]. Indeed, to the best of our knowledge, there are only a few works considering this perspective as briefly discussed in Sect. 1. At the same time, it is unclear how such countermeasures would be implemented or the implementation cost.

4 the RL-Based Countermeasure Selection Framework

4.1 General Setup

We propose a Tabular Q-Learning algorithm based on MetaQNN that can select countermeasures, including their parameters, to simulate their effectiveness on an existing dataset against an arbitrary neural network. To evaluate the effectiveness of the countermeasures, we use guessing entropy. There are several aspects to consider if using MetaQNN:

1. We need to develop an appropriate reward function that considers particularities of the SCA domain. Thus, considering only machine learning metrics would not suffice.
2. MetaQNN uses a fixed α (learning rate) for Q-Learning while using a learning rate schedule where α decreases either linearly or polynomially are the normal practice [6].

[1] The authors mention they conducted a large number of experiments to find a reward function that works well for different datasets and leakage models, so we decided to use the same reward function.

[2] Many works consider the development of SCA countermeasures, but not specifically against deep learning approaches.

3. One of the shortcomings of MetaQNN is that it requires significant computational power and time to explore the search space properly. As we consider several different countermeasures with its hyperparameters, this results in a very large search space.

We model the selection of the right countermeasures and their parameters as a Markov Decision Process (MDP). Specifically, each state has a transition towards an accepting state with the currently selected countermeasures. Each countermeasure can only be applied once per Q-Learning iteration, so the resulting set of chosen countermeasures can be empty (no countermeasure being added) or contain up to four different countermeasures in any order.[3] One may consider that with the larger number of countermeasures being added to the traces, the more difficult the secret information to be retrieved by the side-channel attacks. However, one should note that the implementation of the countermeasure is not without any cost. Indeed, some software-based countermeasures add overhead in the execution efficiency (i.e., dummy executions), while others add overhead in total power consumption (i.e., dedicated noise engine).

To select optimal countermeasure combinations with a limited burden on the device, a cost function that can approximate the implementation costs should balance the strength of the countermeasure implementation and the security of the device. Thus, such a function is also a perfect candidate as a reward function to guide the Q-learning process. While we try to base the costs on real-world implications of adding each of the countermeasures in a chosen configuration, translating the total cost back to a real-world metric is nontrivial. Therefore, we design a cost function associated with each countermeasure, where the value depends on the chosen countermeasure's configuration. The total cost of the countermeasure set, c_{total}, is defined as:

$$c_{total} = \sum_{i=1}^{|C|} c_i. \tag{3}$$

Here, C represents the set of applied countermeasures, and c_i is the cost of the individual countermeasure defined differently for each countermeasure. Based on the values chosen by Wu et al. [26] for the ASCAD fixed key dataset, we set the total cost budget c_{max} to five, but it can be easily adjusted for other implementations. c_{max} set the upper limit of the applied countermeasure so that the selected countermeasure is in a reasonable range and avoid the algorithm to 'cheat' by adding all possible countermeasures with the strongest settings. Only countermeasure configurations within the remaining budget are selectable by the Q-Learning agent. If the countermeasures successfully defeat the attack (GE does not reach 0 within the configured number of attack traces), any leftover budget is used as a component of the reward function. By evaluating the reward function, we can find the best budget-effective countermeasure combinations,

[3] The countermeasures set is an ordered set based on the order that the RL agent selected them. Since the countermeasures are applied in this order, sets with the same countermeasures but a different ordering are treated as disjoint.

together with their settings, to protect the device from the SCA with the lowest budget.

We evaluated four countermeasures: desynchronization, uniform noise, clock jitter, and random delay interrupt (RDI), and applied them to the original dataset. The performance of each countermeasure against deep learning-based SCA can be found in [26]. The countermeasures are all applied a-posteriori to the chosen dataset in our experiments. Note that the implementations of the countermeasure are based on the countermeasure designs from Wu *et al.* [26]. Already that work showed that a combination of countermeasures makes the attack more difficult to succeed.

Some of these countermeasures generate traces of varying length. To make them all of the same length, the traces shorter than the original are padded with zeroes, while any longer traces are truncated back to the original length. The detailed implementation and design of each countermeasure's cost function are discussed in the following sections. We emphasize that the following definitions of the countermeasure cost are customized for the selected attack datasets. They can be easily tuned and adjusted to other implementations based on the actual design specifications.

Desynchronization We draw a number uniformly between 0 and the chosen maximum desynchronization for each trace in the dataset and shift the trace by that number of features. In terms of the cost for desynchronization, Wu *et al.* showed that a maximum desynchronization of 50 greatly increases the attack's difficulty. This leads us to set the desynchronization level ($desync\_level$) ranges from 5 to 50 in a step of 5 (thus, not allowing the desynchronization value so large that it will be trivial to defeat the deep learning attack). The cost calculation for desynchronization is defined in Eq. (4). Note that the maximum c_{desync} is five, which matches the c_{max} we defined as the total cost of countermeasures (which is why c_{desync} needs to be divided by ten).

$$c_{desync} = \frac{desync\_level}{10}. \tag{4}$$

Uniform Noise. Several sources, such as the transistor, data buses, the transmission line to the record devices such as oscilloscopes, or even the work environment, introduce noise to the amplitude domain. Adding uniform noise amounts to adding a uniformly distributed random value to each feature. To make sure the addition of the noise causes a similar effect on different datasets, we set the maximum $noise\_level$ based on the dataset variation defined by Eq. (5):

$$max\_noise\_level = \frac{\sqrt{Var(T)}}{2}. \tag{5}$$

Here, T denotes the measured leakage traces. Then, max_noise_level is multiplied with a $noise\_factor$ parameter, ranging from 0.1 to 1.0 with steps of 0.1, to control the actual noise level introduced to the traces. Since the $noise\_factor$

is the only adjustable parameter, we define the cost of the uniform noise in Eq. (6) to make sure that the maximum c_{noise} equals to c_{max}.

$$c_{noise} = noise\_factor \times 5. \tag{6}$$

Clock Jitter. One way of implementing clock jitters is by introducing the instability in the clock [3]. While desynchronization introduces randomness globally in the time domain, the introduction of clock jitters increases each sampling point's randomness, thus increasing the alignment difficulties. When applying the clock jitter countermeasure to the ASCAD dataset, Wu *et al.* chose eight as the jitter level, but none of the attacks managed to retrieve the key in 10 000 traces. Thus, we decide to tune the jitter level ($jitter\_level$) with a maximum of eight. The corresponding cost function is defined in Eq. 7. In the following experiments, we set the $jitter\_level$ ranging from 2 to 8 in a step of 2. Again, maximum c_{jitter} value matches the c_{max} value we defined before.

$$c_{jitter} = jitter\_level \times 1.6. \tag{7}$$

Random Delay Interrupts (RDIs) Similar to clock jitter, RDIs introduce local desynchronization in the traces. We implement RDIs based on the floating mean method [5]. More specifically, we add RDI for each feature in each trace with a configurable probability. If an RDI occurs for a trace feature, we select the delay length based on the A and B parameters, where A is the maximum length of the delay and B is a number $\leqslant A$. Since RDIs in practice are implemented using instructions such as *nop*, we do not simply flatten the simulated power consumption but introduce peaks with a configurable amplitude. Since the RDI countermeasure has many adjustable parameters, it will, by far, have the most MDP paths dedicated to it, meaning that during random exploration, it is far more likely to select it as a countermeasure. To offset this, we reduce the number of configurable parameters by fixing the amplitude for RDIs based on the max_noise_level defined in Eq. 5 for each dataset. Furthermore, we add 1 to the cost of any random delay interrupt countermeasure, as shown in Eq. 8, defining the cost function for RDIs.

$$c_{rdi} = 1 + \frac{3 \times probability \times (A + B)}{2}, \tag{8}$$

where A ranges from 1 to 10, B ranges from 0 to 9, and $probability$ ranges from 0.1 to 1 in a step of 1. We emphasize that we made sure the selected B value is never larger than A.

When looking at the parameters Wu *et al.* [26] used for random delay interrupts applied on the ASCAD fixed key dataset, $A = 5$, $B = 3$ and $probability = 0.5$, none of the chosen attack methods show any signs of converging on the correct key guess, even after 10 000 traces. With our chosen c_{rdi}, this configuration cost equals seven, which we consider appropriate.

We emphasize that we selected the ranges for each countermeasure based on the related works, while the cost of such countermeasures is adjusted based on the maximum allowed budget. While these values are indeed arbitrary, they can be easily adjusted for any real-world setting. We do not give to each countermeasure the same cost, but normalize it so that the highest value for each countermeasure represents a setting that is difficult to break and consumes the whole cost budget.

4.2 Reward Functions

To allow MetaQNN to be used for the countermeasure selection, we use a relatively complex reward function. This reward function incorporates the guessing entropy and is composed of four metrics: 1) t': the percentage of traces required to get the GE to 0 out of the fixed maximum attack set size; 2) GE'_{10}: the GE value using 10% of the attack traces; 3) GE'_{50}: the GE value using 50% of the attack traces and 4) c': the percentage of countermeasures budget left over out of the fixed maximum budget parameter. The formal definitions of the first three metrics are expressed in Eqs. (9), (10), (11), and (12). We note this is the same reward function as used in [20].

$$t' = \frac{t_{max} - min(t_{max},\ \overline{Q}_{t_{GE}})}{t_{max}}. \tag{9}$$

$$GE'_{10} = \frac{128 - min(GE_{10}, 128)}{128}. \tag{10}$$

$$GE'_{50} = \frac{128 - min(GE_{50}, 128)}{128}. \tag{11}$$

$$c' = \frac{c_{max} - c_{total}}{c_{max}}. \tag{12}$$

The first three metrics of the reward function are derived from the GE metric, aiming to reward neural network architectures based on their attack performance using the configured number of attack traces.[4] Since we reward countermeasure sets that manage to reduce the SCA performance, we incorporate the inverse of these metrics into our reward functions, as these metrics are appropriate in a similar setting [20]. Combining these three metrics allows us to assess the countermeasure set performance, even if the neural network model does not retrieve the secret key within the maximum number of attack traces. We incorporate these metrics inversely into our reward function by subtracting their value from their maximum value. Combined, the sum of the maximum values from which we subtract (multiplied by their weight in the reward function) equals 2.5, as

[4] Note that the misleading GE behavior as discussed in [27] may happen during the experiments. Although one could reverse the ranking provided by an attack to obtain the correct key, we argue it is not possible in reality as an attacker would always assume the correct key being the one with the lowest GE (most likely guess).

shown in Eq. (13). The weight of each metric is determined based on a large number of experiments.

In terms of the fourth metric c', recall C is the set of countermeasures chosen by the agent, and c_{total} equals five. We only apply this reward when the key retrieval is unsuccessful in t_{max} traces, as we do not want to reward small countermeasure sets for their size if they do not adequately decrease the attack performance. Combining these four metrics, we define the reward function as in Eq. (13), which gives us a total reward between 0 and 1. To better reward the countermeasure set performance, making the SCA neural networks require more traces for a successful break, a smaller weight is set on GE'_{50}.

$$R = \frac{1}{3} \times \begin{cases} 2.5 - t' - GE'_{10} - 0.5 \times GE'_{50}, & \text{if } t_{GE=0} < t_{max} \\ 2.5 - GE'_{10} - 0.5 \times GE'_{50} + 0.5 \times c', & \text{otherwise} \end{cases} \tag{13}$$

We multiply the entire set of metrics by $\frac{1}{3}$ to normalize our reward function between 0 and 1. While this reward function does look complicated, it is derived based on the results from [20] and our experimental tuning lasting several weeks. Still, we do not claim the presented reward function is optimal, but it gives good results. Further improvements are always possible, especially from the budget perspective or the cost of a specific countermeasure.

5 Experimental Results

To assess the performance of the selected set of countermeasures for each dataset and leakage model, we perform experiments with different CNN models (as those are reported to reach top results in SCA, see, e.g. [10,29]). Those models are tuned for each dataset and leakage model combination without considering hiding countermeasures that we simulate. One could consider this not to be fair as those architectures do not necessarily work well with countermeasures. Still, there are two reasons to follow this approach as we 1) do not know a priori the best set of countermeasures and we do not want to optimize both architectures and countermeasures at the same time, and 2) evaluate against state-of-the-art architectures that are not tuned against any of those countermeasures to allow a fair assessment of all architectures.

Specifically, we use reinforcement learning to select the model's hyperparameter [20]. We execute the search algorithm for every dataset and leakage model combination and select the top-performing models over 2 500 iterations. To assess the performance of the Q-Learning agent, we compare the average rewards per ε. For instance, a ε of 1.0 means the network was generated completely randomly, while an ε of 0.1 means that the network was generated while choosing random actions 10% of the time. For the test setup, we use an NVIDIA GTX 1080 Ti graphics processing unit (GPU) with 11 Gigabytes of GPU memory and 3 584 GPU cores. All of the experiments are implemented with the TensorFlow [1] computing framework and Keras deep learning framework [4].

The details about the specific architectures can be found in Table 1. Note that Rijsdijk *et al.* implemented two reward functions: one that only considers the attack performance, and the other that also considers the network size (small reward function) [20]. We consider both reward functions aligned with that paper, leading to two models used for testing; the one denoted with RS is the model optimized with the small reward function. For all models, we use $he\_uniform$ and $selu$ as kernel initializer and activation function.

Table 1. CNN architectures used in the experiments [20].

Test models	Convolution (filter_number, size)	Pooling (size, stride)	Fully-connected layer
$ASCAD_{HW}$	Conv(16, 100)	avg(25, 25)	15+4+4
$ASCAD_{HW\_RS}$	Conv(2, 25)	avg(4, 4)	15+10+4
$ASCAD_{ID}$	Conv(128, 25)	avg(25, 25)	20+15
$ASCAD_{ID\_RS}$	Conv(2+2+8, 75+3+2)	avg(25+4+2, 25+4+2)	10+4+2
$ASCAD\_R_{HW}$	Conv(4, 50)	avg(25, 25)	30+30+30
$ASCAD\_R_{HW\_RS}$	Conv(8, 3)	avg(25, 25)	30+30+20
$ASCAD\_R_{ID}$	Conv(128, 3)	avg(75, 75)	30+2
$ASCAD\_R_{ID\_RS}$	Conv(4, 1)	avg(100, 75)	30+10+2

5.1 ASCAD Fixed Key Dataset

Figure 1 shows the scatter plot results for the HW and ID leakage models for both the regular and RS CNN. The vertical red line indicates the highest Q-learning reward for the countermeasure set, which could not prevent the CNN from retrieving the key within the configured 2 000 attack traces. Notably, a sharp line can be found on the right side of the Q-Learning reward plots, which is solely due to the c' component of the reward function. Although the selected CNNs can retrieve the secret key when no countermeasures were applied ($c' = 0$) for all experiments with both HW and ID leakage models, as soon as any countermeasure is applied, the attack becomes unsuccessful with 2 000 attack traces. Indeed, we observe that only very few countermeasures seem inefficient in defeating the deep learning attacks from the result plots.

For the experiments presented, the top countermeasures for ASCAD using different profiling models are listed in Table 2. Notably, the best countermeasure set in terms of performance and cost for this CNN consists of desynchronization with a level equal to ten, which could be caused by the lack of sufficient convolution layers (only one) in countering such a countermeasure. The rest of the top 20 countermeasure sets include or solely consist of random delay interrupts. This observation is also applied to other profiling models and ID leakage models. The amplitude for RDI is fixed for each dataset, as explained in Sect. 4.1. In terms of the parameters of RDIs, B stays zero for all three profiling models, indicating that A solely determines the length of RDIs. Indeed, B varies the mean of the number of added RDIs and enhances the difficulties in learning from the data. However, a larger B value would also increase the countermeasure cost, which is against the reward function's principle. From Table 2, we can observe both low values of A and *probability* being applied to the RDIs countermeasure, indicating the success of our framework in finding countermeasure with high performance and low cost.

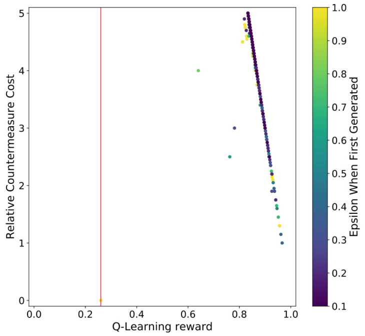

(a) ASCAD fixed key HW leakage model (192 hours).

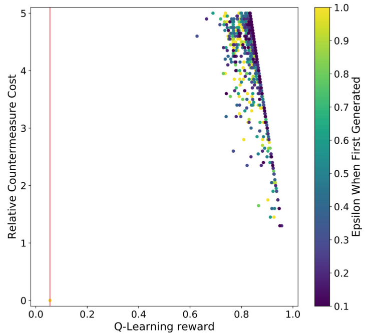

(b) ASCAD fixed key ID leakage model (204 hours).

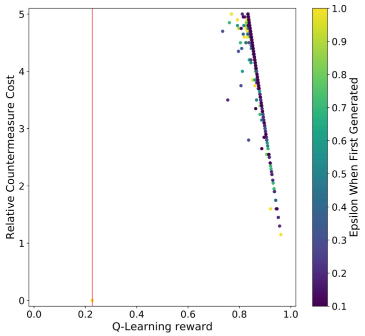

(c) ASCAD fixed key HW leakage model (RS) (196 hours).

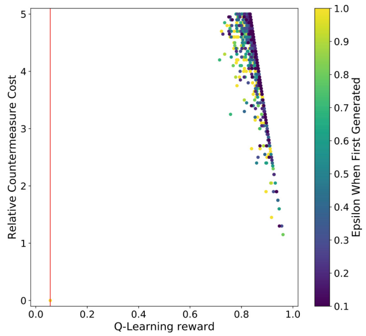

(d) ASCAD fixed key ID leakage model (RS) (198 hours).

Fig. 1. An overview of the countermeasure cost, reward, and the ε value a countermeasure combination set was first generated for the ASCAD with fixed key dataset experiments. The red lines indicate the countermeasure set with the highest reward for that GE reached 0 within 2 000 traces. (Color figure online)

Next, we compare the general performance of the countermeasure sets between CNNs designed for the HW and ID leakage model. We observe that the ID model appears to be at least a little better at handling countermeasures. Specifically, for the ID leakage model CNNs, the countermeasures' Q-Learning reward variance is higher, indicating that the ID model CNNs can better handle countermeasures, making the countermeasure selection more important. This

Table 2. Best performing countermeasures for the ASCAD fixed key dataset.

Model	Reward	Countermeasures	c'
$ASCAD_{HW}$	0.967	Desync(desync_level = 10)	1.00
$ASCAD_{HW\_RS}$	0.962	RDI(A = 1, B = 0, probability = 0.10, amplitude = 12.88)	1.15
$ASCAD_{ID}$	0.957	RDI(A = 2, B = 0, probability = 0.10, amplitude = 12.88)	1.30
$ASCAD_{ID\_RS}$	0.962	RDI(A = 1, B = 0, probability = 0.10, amplitude = 12.88)	1.15

observation is confirmed by the c' value listed in Table 2: to reach a similar level of the reward value, the countermeasures are implemented with a greater cost.

Considering the time required to run the reinforcement learning, we observe we require around 200 h on average, which is double the time required by Rijsdijk et al. when finding neural networks that perform well [20]. In Fig. 2, we show the rolling average of the Q-learning reward and the average Q-learning reward per epsilon for the ASCAD fixed key dataset. As can be seen, the reward value for countermeasure gradually increases when more iteration is performed, indicating that the agent is learning from the environment and becoming more capable of finding effective countermeasure settings with a low cost. Then, the reward value is saturated when ε reaches 0.1, meaning that the agent is well trained and constantly finds well-performing countermeasures. One may notice that the number of iterations performed is significantly higher than the configured 1 700 iterations. This is because we only count an iteration when generating a countermeasure set that was not generated before.

5.2 ASCAD Random Keys Dataset

The scatter plot results for both the HW and ID model for both the regular and RS CNN are listed in Fig. 3. Aligned with the ASCAD fixed key dataset observation, the vertical red line in the plots is far away from the dots in the plot, indicating that the countermeasure's addition effectively increases side-channel attack difficulty. Furthermore, we again see the sharp line on the right side of the Q-Learning reward, which is caused by the c' component of the reward function.

Compared with the ASCAD results for both leakage models (Fig. 1), we see a greater variation of the individual countermeasure implementations: even with the same countermeasure cost, a different combination of countermeasures and their corresponding setting may lead to unpredictable reward values. Fortunately, we see this tendency with the RL-based countermeasure selection scheme and can better select the countermeasures' implementation with a limited budget. Finally, we observe that the later leakage model is more effective in defeating the countermeasure when comparing the HW and ID leakage models. In other words, to protect the essential execution that leaks the ID information, more effort may be required to implement countermeasures. The top-performing countermeasures for different profiling models are listed in Table 3. From the results, RDIs again become the most effective one among all of the considered countermeasures. The RDI amplitude is fixed at 16.95 for this dataset, as explained in Sect. 4.1.

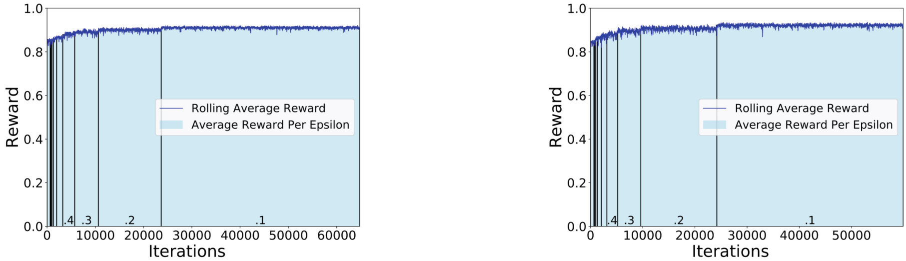

(a) ASCAD fixed key HW leakage model.

(b) ASCAD fixed key ID leakage model.

Fig. 2. An overview of the Q-Learning performance for the ASCAD with fixed key dataset experiments. The blue line indicates the rolling average of the Q-Learning reward for 50 iterations, where at each iteration, we generate and evaluate a countermeasure set. The bars in the graph indicate the average Q-Learning reward for all countermeasure sets generated during that ε. The results for RS experiments are similar. (Color figure online)

Interestingly, the countermeasures are implemented with higher costs when compared with the one used for ASCAD with a fixed key. The reason could be that training with random keys traces enhances the generalization of the profiling model. What is more, we also observe that we require significantly longer time to run the reinforcement learning framework: on average, 300 h, which is more than 12 days of computations. Interestingly, we see an outlier with the ASCAD random keys for the ID leakage model, where only 48 h were needed for the experiments.

Table 3. Best performing countermeasures for the ASCAD random keys dataset.

Model	Reward	Countermeasures	c'
$ASCAD\_R_{HW}$	0.940	RDI(A = 1, B = 0, probability = 0.20, amplitude = 16.95)	1.30
$ASCAD\_R_{HW\_RS}$	0.952	RDI(A = 2, B = 1, probability = 0.10, amplitude = 16.95)	1.45
$ASCAD\_R_{ID}$	0.942	RDI(A = 5, B = 0, probability = 0.10, amplitude = 16.95)	1.75
$ASCAD\_R_{ID\_RS}$	0.962	RDI(A = 1, B = 0, probability = 0.10, amplitude = 16.95)	1.15

The rolling average of the Q-learning reward and the average Q-learning reward per ε for the ASCAD random keys dataset are given in Fig. 4, Appendix A. Interestingly, at the beginning of Fig. 4a, there is a significant drop in Q-learning reward, followed by a rapid increase in the ε update from 0.4 to 0.3. A possible explanation could be that the model we used is powerful in defeating the selected countermeasures at the early learning stage. Still, the algorithm managed to learn from each interaction, finally selecting powerful countermeasures. In contrast, selecting countermeasure to defeat $ASCAD\_R_{ID}$ is an easy task: the reward value reaches above 0.8 at the very beginning, and it

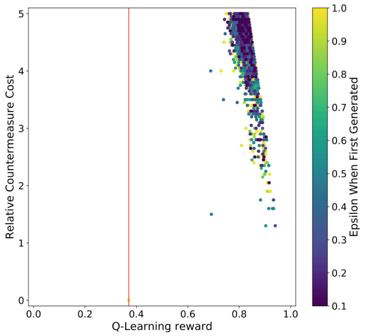

(a) ASCAD random keys HW leakage model (280 hours).

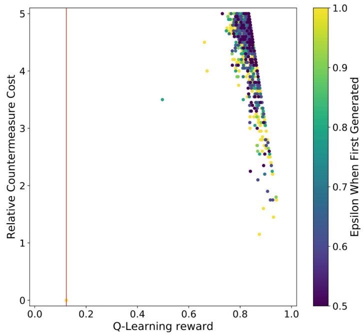

(b) ASCAD random keys ID leakage model (48 hours).

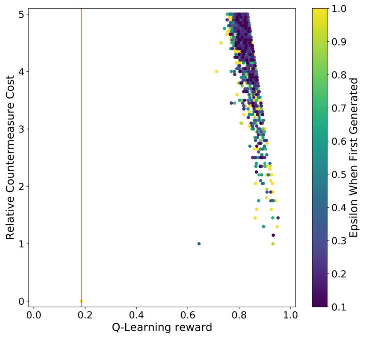

(c) ASCAD random keys HW leakage model (RS) (296 hours).

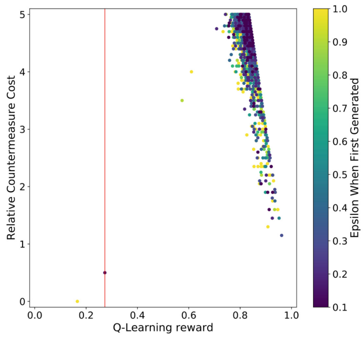

(d) ASCAD random keys ID leakage model (RS) (309 hours).

Fig. 3. An overview of the countermeasure cost, reward, and the ε value a countermeasure combination set was first generated for the ASCAD with random keys dataset experiments. The red lines indicates the countermeasure set with the highest reward for that GE reached 0 within 2 000 traces. (Color figure online)

stops increasing regardless of the number of iterations. Since each test consumes 300 h on average, we stopped the tests after around 3 000 iterations. There is a similar performance for settings with the RS objective in the ASCAD with the fixed key dataset: the RL algorithm is constantly learning. The highest reward value is obtained when ε reaches the minimum.

6 Conclusions and Future Work

This paper presents a novel approach to designing side-channel countermeasures based on reinforcement learning. We consider four well-known types of countermeasures (one in the amplitude domain and three in the time domain), and we aim to find the best combinations of countermeasures within a specific budget. We conduct experiments on two datasets and report a number of countermeasure combinations providing significantly improved resilience against deep learning-based SCA. Our experiments show that the best performing countermeasure combinations use the random delay interrupt countermeasure, making it a natural choice for real-world implementations. While the specific cost for each countermeasure was defined arbitrarily (as well as the total budget), we believe the whole approach is easily transferable to settings with real-world targets.

The experiments performed currently take significantly longer than might be necessary, as we generate a fixed number of unique countermeasure sets. In contrast, the chance to generate a unique countermeasure set towards the end of the experiments is significantly smaller (due to the lower ε). For future work, we plan to explore how to detect this behavior. Besides, it would be interesting to benchmark our method with Dynamic Programming or random solutions. We plan to consider multilayer perceptron architectures and sets of countermeasures that work well for different datasets and leakage models. Moreover, this work only evaluates existing countermeasures. It would also be interesting to investigate if reinforcement learning can be used to develop novel countermeasures.

A Q-Learning Performance for the ASCAD with Random Keys Dataset

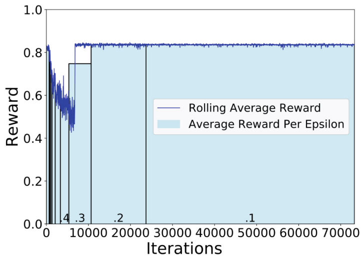

(a) ASCAD random keys HW leakage model.

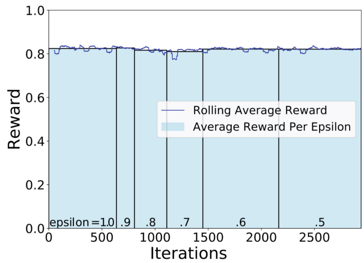

(b) ASCAD random keys ID leakage model.

Fig. 4. An overview of the Q-Learning performance for the ASCAD with the random keys dataset experiments. The blue line indicates the rolling average of the Q-Learning reward for 50 iterations, where at each iteration, we generate and evaluate a countermeasure set. The bars in the graph indicate the average Q-Learning reward for all countermeasure sets generated during that ε. The results for RS experiments are similar. (Color figure online)

References

1. Abadi, M., et al.: TensorFlow: large-scale machine learning on heterogeneous systems (2015). http://tensorflow.org/, software available from tensorflow.org

2. Benadjila, R., Prouff, E., Strullu, R., Cagli, E., Dumas, C.: Deep learning for side-channel analysis and introduction to ASCAD database. J. Cryptogr. Eng. **10**(2), 163–188 (2020). https://doi.org/10.1007/s13389-019-00220-8
3. Cagli, E., Dumas, C., Prouff, E.: Convolutional neural networks with data augmentation against jitter-based countermeasures. In: Fischer, W., Homma, N. (eds.) CHES 2017. LNCS, vol. 10529, pp. 45–68. Springer, Cham (2017). https://doi.org/10.1007/978-3-319-66787-4_3
4. Chollet, F., et al.: Keras (2015). https://github.com/fchollet/keras
5. Coron, J.-S., Kizhvatov, I.: An efficient method for random delay generation in embedded software. In: Clavier, C., Gaj, K. (eds.) CHES 2009. LNCS, vol. 5747, pp. 156–170. Springer, Heidelberg (2009). https://doi.org/10.1007/978-3-642-04138-9_12
6. Even-Dar, E., Mansour, Y.: Learning rates for q-learning. J. Mach. Learn. Res. **5**, 1–25 (2004)
7. Gu, R., Wang, P., Zheng, M., Hu, H., Yu, N.: Adversarial attack based countermeasures against deep learning side-channel attacks (2020)
8. Hettwer, B., Gehrer, S., Güneysu, T.: Deep neural network attribution methods for leakage analysis and symmetric key recovery. In: Paterson, K.G., Stebila, D. (eds.) SAC 2019. LNCS, vol. 11959, pp. 645–666. Springer, Cham (2020). https://doi.org/10.1007/978-3-030-38471-5_26
9. Inci, M.S., Eisenbarth, T., Sunar, B.: Deepcloak: Adversarial crafting as a defensive measure to cloak processes. CoRR abs/1808.01352 (2018). http://arxiv.org/abs/1808.01352
10. Kim, J., Picek, S., Heuser, A., Bhasin, S., Hanjalic, A.: Make some noise. unleashing the power of convolutional neural networks for profiled side-channel analysis. IACR Trans. Cryptogr. Hardw. Embed. Syst. 148–179 (2019)
11. Maghrebi, H., Portigliatti, T., Prouff, E.: Breaking cryptographic implementations using deep learning techniques. In: Carlet, C., Hasan, M.A., Saraswat, V. (eds.) SPACE 2016. LNCS, vol. 10076, pp. 3–26. Springer, Cham (2016). https://doi.org/10.1007/978-3-319-49445-6_1
12. Masure, L., Dumas, C., Prouff, E.: Gradient visualization for general characterization in profiling attacks. In: Polian, I., Stöttinger, M. (eds.) COSADE 2019. LNCS, vol. 11421, pp. 145–167. Springer, Cham (2019). https://doi.org/10.1007/978-3-030-16350-1_9
13. Ouytsel, C.B.V., Bronchain, O., Cassiers, G., Standaert, F.: How to fool a black box machine learning based side-channel security evaluation. Cryptogr. Commun. **13**(4), 573–585 (2021). https://doi.org/10.1007/s12095-021-00479-x
14. Perin, G., Chmielewski, L., Picek, S.: Strength in numbers: improving generalization with ensembles in machine learning-based profiled side-channel analysis. IACR Trans. Cryptogr. Hardw. Embed. Syst. **2020**(4), 337–364 (2020). https://doi.org/10.13154/tches.v2020.i4.337-364, https://tches.iacr.org/index.php/TCHES/article/view/8686
15. Perin, G., Picek, S.: On the influence of optimizers in deep learning-based side-channel analysis. In: Dunkelman, O., Jacobson, Jr., M.J., O'Flynn, C. (eds.) SAC 2020. LNCS, vol. 12804, pp. 615–636. Springer, Cham (2021). https://doi.org/10.1007/978-3-030-81652-0_24
16. Perin, G., Wu, L., Picek, S.: Gambling for success: The lottery ticket hypothesis in deep learning-based sca. Cryptology ePrint Archive, Report 2021/197 (2021). https://eprint.iacr.org/2021/197

17. Picek, S., Heuser, A., Jovic, A., Bhasin, S., Regazzoni, F.: The curse of class imbalance and conflicting metrics with machine learning for side-channel evaluations. IACR Trans. Cryptogr. Hardw. Embed. Syst. **2019**(1), 209–237 (2018). https://doi.org/10.13154/tches.v2019.i1.209-237, https://tches.iacr.org/index.php/TCHES/article/view/7339
18. Picek, S., Jap, D., Bhasin, S.: Poster: when adversary becomes the guardian - towards side-channel security with adversarial attacks. In: Proceedings of the 2019 ACM SIGSAC Conference on Computer and Communications Security, pp. 2673–2675. CCS 2019, Association for Computing Machinery, New York, NY, USA (2019). https://doi.org/10.1145/3319535.3363284
19. Ramezanpour, K., Ampadu, P., Diehl, W.: SCARL: side-channel analysis with reinforcement learning on the Ascon authenticated cipher (2020)
20. Rijsdijk, J., Wu, L., Perin, G., Picek, S.: Reinforcement learning for hyperparameter tuning in deep learning-based side-channel analysis. IACR Trans. Cryptogr. Hardw. Embed. Syst. **2021**(3), 677–707 (2021). https://doi.org/10.46586/tches.v2021.i3.677-707, https://tches.iacr.org/index.php/TCHES/article/view/8989
21. Standaert, F.-X., Malkin, T.G., Yung, M.: A unified framework for the analysis of side-channel key recovery attacks. In: Joux, A. (ed.) EUROCRYPT 2009. LNCS, vol. 5479, pp. 443–461. Springer, Heidelberg (2009). https://doi.org/10.1007/978-3-642-01001-9_26
22. Sutton, R.S., Barto, A.G.: Reinforcement Learning: An Introduction, 2 edn. MIT Press, Cambridge (2018). http://incompleteideas.net/book/the-book.html
23. Watkins, C.J.C.H.: Learning from delayed rewards. Phd thesis, University of Cambridge England (1989)
24. Wouters, L., Arribas, V., Gierlichs, B., Preneel, B.: Revisiting a methodology for efficient CNN architectures in profiling attacks. IACR Trans. Cryptogr. Hardw. Embed. Syst. **2020**(3), 147–168 (2020). https://doi.org/10.13154/tches.v2020.i3.147-168, https://tches.iacr.org/index.php/TCHES/article/view/8586
25. Wu, L., Perin, G., Picek, S.: I choose you: automated hyperparameter tuning for deep learning-based side-channel analysis. Cryptology ePrint Archive, Report 2020/1293 (2020). https://eprint.iacr.org/2020/1293
26. Wu, L., Picek, S.: Remove some noise: On pre-processing of side-channel measurements with autoencoders. IACR Trans. Cryptogr. Hardw. Embed. Syst. **2020**(4), 389–415 (2020). https://doi.org/10.13154/tches.v2020.i4.389-415, https://tches.iacr.org/index.php/TCHES/article/view/8688
27. Wu, L., et al.: On the attack evaluation and the generalization ability in profiling side-channel analysis. Cryptology ePrint Archive, Report 2020/899 (2020). https://eprint.iacr.org/2020/899
28. Zaid, G., Bossuet, L., Dassance, F., Habrard, A., Venelli, A.: Ranking loss: maximizing the success rate in deep learning side-channel analysis. IACR Trans. Cryptogr. Hardw. Embed. Syst. **2021**(1), 25–55 (2021). https://doi.org/10.46586/tches.v2021.i1.25-55
29. Zaid, G., Bossuet, L., Habrard, A., Venelli, A.: Methodology for efficient cnn architectures in profiling attacks. IACR Trans. Cryptogr. Hardw. Embed. Syst.**2020**(1), 1–36 (2019). https://doi.org/10.13154/tches.v2020.i1.1-36, https://tches.iacr.org/index.php/TCHES/article/view/8391
30. Zhang, J., Zheng, M., Nan, J., Hu, H., Yu, N.: A novel evaluation metric for deep learning-based side channel analysis and its extended application to imbalanced data. IACR Trans. Cryptogr. Hardw. Embed. Syst. **2020**(3), 73–96 (2020). https://doi.org/10.13154/tches.v2020.i3.73-96, https://tches.iacr.org/index.php/TCHES/article/view/8583